

# Affinity Proteomic Profiling of Plasma, Cerebrospinal Fluid, and Brain Tissue within Multiple Sclerosis

Sanna Byström,<sup>†,‡</sup> Burcu Ayoglu,<sup>†,‡</sup> Anna Häggmark,<sup>†</sup> Nicholas Mitsios,<sup>‡</sup> Mun-Gwan Hong,<sup>†</sup> Kimi Drobis,<sup>†</sup> Björn Forsström,<sup>†</sup> Claudia Fredolini,<sup>†</sup> Mohsen Khademi,<sup>§</sup> Sandra Amor,<sup>||</sup> Mathias Uhlén,<sup>†</sup> Tomas Olsson,<sup>§</sup> Jan Mulder,<sup>‡</sup> Peter Nilsson,<sup>†</sup> and Jochen M. Schwenk\*,<sup>†</sup>

<sup>†</sup>Affinity Proteomics, SciLifeLab, School of Biotechnology, KTH – Royal Institute of Technology, Stockholm 171 21, Sweden

<sup>‡</sup>Department of Neuroscience, SciLifeLab, Karolinska Institute, Stockholm 171 77, Sweden

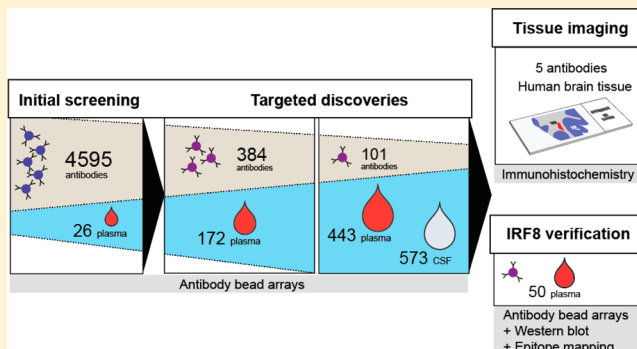
<sup>§</sup>Neuroimmunology Unit, Department of Clinical Neuroscience, Karolinska Institute, Tomtebodavägen 18A, Stockholm 171 77, Sweden

<sup>||</sup>Pathology Department, VU Medical Center, De Boelelaan 1117, Amsterdam 1081 HV, The Netherlands

## Supporting Information

**ABSTRACT:** The brain is a vital organ and because it is well shielded from the outside environment, possibilities for noninvasive analysis are often limited. Instead, fluids taken from the spinal cord or circulatory system are preferred sources for the discovery of candidate markers within neurological diseases. In the context of multiple sclerosis (MS), we applied an affinity proteomic strategy and screened 22 plasma samples with 4595 antibodies (3450 genes) on bead arrays, then defined 375 antibodies (334 genes) for targeted analysis in a set of 172 samples and finally used 101 antibodies (43 genes) on 443 plasma as well as 573 cerebrospinal fluid (CSF) samples. This revealed alteration of protein profiles in relation to MS subtypes for IRF8, IL7, METTL14, SLC30A7, and GAP43. Respective antibodies were subsequently used for immunofluorescence on human post-mortem brain tissue with MS pathology for expression and association analysis. There, antibodies for IRF8, IL7, and METTL14 stained neurons in proximity of lesions, which highlighted these candidate protein targets for further studies within MS and brain tissue. The affinity proteomic translation of profiles discovered by profiling human body fluids and tissue provides a powerful strategy to suggest additional candidates to studies of neurological disorders.

**KEYWORDS:** antibodies, suspension bead arrays, plasma, CSF, brain tissue, immunofluorescence, multiple sclerosis



## INTRODUCTION

Multiple sclerosis (MS) is the most common cause of chronic neurological disability in young adults.<sup>1</sup> It is a neurodegenerative and inflammatory disorder of the central nervous system (CNS), has three major subtypes, and leads to the formation of multifocal demyelinating white matter lesions and gray matter lesions.<sup>2</sup> Although most patients with relapsing remitting MS (RRMS) later develop secondary progressive MS (SPMS), steady progression of neurological damage without periods of remission or recovery from symptoms,<sup>3,4</sup> periods of relapses, and remissions (RR-rel and RR-rem) may persist without worsening of symptoms for years. Current diagnosis of MS currently relies on a combination of several clinical investigations, such as magnetic resonance imaging of the brain and identification of oligoclonal IgG in cerebrospinal fluid (CSF).<sup>5</sup> However, additional indicators of disease are needed because interindividual variations in neuropathological features and clinical manifestations complicate both an early-stage diagnosis and prediction of disease progression.<sup>6,7</sup>

Hereto, proteins in CNS tissue potentially hold much of the sought-after information. However, and as true for other neurological diseases, it is a challenge to access samples of brain tissue for discovery-driven approaches. To otherwise gain insights into disease-related mechanism and pathophysiology, disease-specific protein profiles can be searched for in systemic plasma or proximal CSF.<sup>8–11</sup> The current scarcity of so-far reported disease-specific proteins within MS<sup>12</sup> may be due to several reasons such as the limited number of samples and the aforementioned disease heterogeneity.

Affinity-based assays can be particularly useful to address this challenge because they allow efficient and subsequent use of binding reagents across different analysis platforms and sample

**Special Issue:** Proteomics of Human Diseases: Pathogenesis, Diagnosis, Prognosis, and Treatment

**Received:** June 18, 2014

**Published:** September 18, 2014

materials. Affinity reagents used in the presented study were from the Human Protein Atlas (HPA),<sup>13</sup> which since 2005<sup>14</sup> has produced polyclonal antibodies against more than 80% of all human protein encoding genes and is an initiative aiming to generate affinity reagents for the proteome.<sup>15</sup> Besides using affinity reagents on well-established platforms such as immunohistochemistry, microarray-based assays can be used to screen hundreds of protein targets in hundreds of body fluid samples with minimal requirements on sample volume.<sup>16</sup>

In the presented study, we used affinity proteomic methods to discover MS related protein profiles in body fluids for subsequent tissue analysis. Starting from an initial screening, follow-up and targeted assays were performed on suspension bead arrays for multiplexed profiling of plasma and CSF of MS patients. We then chose the identified targets to study disease processes in sections from human MS brain tissues in combination with markers for astrocytes, microglia, and infiltrating macrophages.

## MATERIALS AND METHODS

### Samples

EDTA plasma samples utilized in the untargeted discovery stage were obtained from an in-house biobank of samples collected during routine neurological diagnostic workup at the neurology clinic of Karolinska University Hospital Stockholm, Sweden. The set of paired plasma and CSF samples utilized in the verification stage contained samples collected at three hospitals within Sweden. All patients were examined and diagnosed by a neurologist and fulfilled the McDonald criteria.<sup>17</sup> Patients with MS were classified as RRMS, SPMS, or primary progressive MS (PPMS), where the first subtype was subdivided further into patients during relapse (RR-rel) or remission (RR-rem). Samples from patients with a single demyelinating event, the so-called clinically isolated syndrome (CIS), were also included in the study. The control group consisted of individuals with other neurological diseases (ONDs) and ONDs with signs of inflammation (iOND). The individuals with OND had a variety of neurological signs and symptoms similar to MS, such as sensory symptoms, visual disturbance, headache, and so on, while the iOND group consisted of individuals with other inflammation-driven diseases such as rheumatoid arthritis (RA), systemic lupus erythematosus (SLE), neuropathy, or viral/bacterial infections, for example, borreliosis, meningitis, or herpes encephalitis (Table 1A–D). Study enrolment followed the recommendations of the Declaration of Helsinki and approval by the Ethics Committee of the Karolinska Institute (DNR 2009/2104-31-2). Oral and written information was given to the patients, and informed consent in writing was received before inclusion. All samples were prepared according to standard procedures and stored at  $-80^{\circ}\text{C}$  until usage.

Tissue brain sections from 15 patients with MS were obtained from tissues collected at autopsy, and patient characteristics are listed in Supplementary Table 1 in the Supporting Information. The rapid autopsy regimen of The Netherlands Brain Bank in Amsterdam (coordinated by Dr. I. Huitinga) was used to acquire the samples, with the approval of the Medical Ethical Committee of the VU University Medical Center. All patients and controls had given informed consent for autopsy and use of their brain tissue for research purposes. All patient material was coded to ensure anonymity throughout tissue processing. The clinical neuropathological diagnosis for

**Table 1. (A) Demographics of Plasma Samples Used for Targeted Discovery, (B) Demographics of Plasma Samples Used for Verification, (C) Demographics of CSF Specimen, and (D) Demographics of Plasma Samples Used for IRF8 Verification**

sample group	N	% female	(A)	
			median	age range
OND	64	67	40	19–68
CIS-rem	13	62	33	25–60
CIS-rel	5	80	51	37–63
RR-rem	46	74	32	19–57
RR-rel	14	57	29	22–56
SPMS	20	70	52	35–68
PPMS	10	60	52	44–62
<b>total</b>	<b>172</b>			
sample group	N	% female	(B)	
			median	age range
OND	101	72	41	19–68
iOND	83	72	43	18–83
CIS-rem	28	75	34	21–60
CIS-rel	11	82	37	23–63
RR-rel	147	74	39	17–70
RR-rem	38	55	38	22–60
SPMS	35	54	54	28–68
<b>total</b>	<b>443</b>			
sample group	N	% female	(C)	
			median	age range
iOND	91	72	41	18–83
OND	148	74	40	19–68
CIS-rem	11	82	37	23–63
CIS-rel	31	77	33	21–60
RR-rem	42	62	40	22–68
RR-rel	193	75	38	17–70
SPMS	43	53	54	35–68
PPMS	14	64	52	35–62
<b>total</b>	<b>573</b>			
sample group	N	% female	(D)	
			median	age range
CIS	17	82	37	25–50
RR-rem	17	74	37	25–50
SPMS	16	60	47	33–61
<b>total</b>	<b>50</b>			

MS tissues was confirmed by Prof. P. van der Valk. Tissue samples from MS cases were obtained after ex vivo magnetic resonance imaging scanning, as previously described by De Groot et al.<sup>18</sup> Classification of lesion staging was based on immunohistochemical detection of cells that express major histocompatibility complex (MHC) class II/HLA-DR and the presence of proteolipid protein (PLP) to reveal areas of myelin loss.<sup>18</sup> A set of healthy control human brains from patients who had no infections or history of serious illness or head trauma was obtained from the Department of Immunology, Genetics and Pathology, SciLifeLab Uppsala, Stockholm.<sup>19</sup>

### Antibodies and Bead Array Generation

The majority of the antibodies utilized in this study were generated within the Human Protein Atlas project, as

previously described,<sup>20</sup> and additional antibodies were obtained through various commercial sources (see Supplementary Table 2 in the Supporting Information). Antibodies for the initial plasma screening were not selected based on their target protein but as they became available from the Human Protein Atlas.<sup>21</sup> However, in the targeted screening, the selection was made based on prior knowledge of disease relation according to literature and in-house multidisease studies including other neurodegenerative diseases (Alzheimer's disease, Parkinson's disease, amyotrophic lateral sclerosis, and mild cognitive impairment).

Bead arrays were created as previously described<sup>22</sup> with modifications that relate to normalizing the concentration of antibodies using liquid handling (EVO150, TECAN) by diluting 1.6 µg of each antibody into 100 µL of 0.05 M MES buffer (pH 4.5). All antibodies were then coupled to carboxylated, color-coded magnetic beads (MagPlex-C, Luminex) to create bead arrays of up to 384-plex. The coupling of each antibody on the beads was confirmed via R-phycerythrin-conjugated donkey antirabbit IgG antibody (Jackson ImmunoResearch), where all antibodies revealed median fluorescence intensity (MFI) values of 15 000–19 000 AU.

### Plasma Profiling

Plasma samples stored at –80 °C were thawed at 4 °C, centrifuged for 10 min at 3000 rpm, and then transferred into 96-well microtiter plates with a liquid handling system (EVO150, TECAN). Sample locations were randomized according to a plate layout design, which allowed a balanced distribution of samples across multiple plates in terms of both categorical variables and the quantitative variable of age. Samples were then labeled with biotin, as previously described<sup>23</sup> and transferred by liquid handling (Selma, CyBio). The 1:10 diluted and biotinylated samples were subsequently utilized without removal of excess biotin and diluted 1:50 in an assay buffer composed of 0.5% (w/v) poly(vinyl alcohol) and 0.8% (w/v) polyvinylpyrrolidone (Sigma) in 0.1% casein in PBS (PVXC) supplemented with 0.5 mg/mL nonspecific rabbit IgG (Bethyl), yielding a total sample dilution of 1:500. Diluted samples were heat-treated for 30 min at 56 °C and cooled to 20 °C for 15 min in a thermocycler (Techne, TC-PLUS), and 45 µL of heat-treated samples was added to 5 µL of the antibody suspension bead array distributed into a 384-well microtiter plate (Greiner BioOne). The incubation took place overnight on a shaker (Grant) at ambient temperature. Beads were then washed with 3 × 60 µL PBS-T (1 × PBS pH 7.4, 0.05% Tween20) using a plate washer (EL406, Bioteck), followed by an incubation for 10 min with 50 µL of a stop solution containing 0.4% paraformaldehyde in PBS. Beads were washed with 1 × 60 µL of PBS-T, and 50 µL of 0.5 µg/mL R-phycerythrin-labeled streptavidin (Invitrogen) in PBS-T was added and incubated for 20 min. Finally, beads were washed with 3 × 60 µL and measured in 60 µL of PBS-T. Measurements were performed using a FlexMap3D instrument (Luminex). For each sample and bead ID, 50 events were collected, and binding to beads was reported as MFI and used for data analysis.

### CSF Profiling

Immediately after lumbar puncture, cells were removed from CSF supernatant by centrifugation at 350g, and samples were frozen at –80 °C. As previously described,<sup>23</sup> all CSF samples were diluted 1:2 in PBS supplemented with 0.5% BSA (Sigma) and 0.1% rabbit IgG (Bethyl) at labeling, where a 10-fold molar

excess of biotin over protein amount was utilized. Before incubation with the antibody bead array, samples were diluted 1:8 in PVXC buffer, heat-treated at 56 °C for 30 min, and cooled to 20 °C for 15 min. Incubation and the following sample processing was performed according to the described plasma procedure.

### Western Blot Analysis

A plasma pool from four MS patients and IRF8 overexpressing lysate (LY419485, OriGene) was diluted 1:50 and 1:100 in LDS sample buffer and sample reducing agent (both from NuPAGE Invitrogen) dissolved in Milli-Q water. Samples were heated to 95 °C for 5 min, loaded on a Bis-Tris 4–12% gel (Invitrogen) and run at constant 200 V using a XCell SureLock mini-cell electrophoresis system (Invitrogen) with MOPS SDS running buffer (Invitrogen). A Novex X-Cell II blot module (Invitrogen) was used for transferring proteins onto a 0.45 µm PVDF membrane (Invitrogen) at constant 30 V. Membranes were blocked with blocking reagents for ELISA for 2 h prior overnight incubation at 4 °C with primary antibodies (1 µg/mL). Membranes were washed three times in TBS-T (1 × TBS pH 7.5, 0.05% Tween20) and detection was enabled using HRP-labeled antirabbit, antimouse (both Dako), and antisheep antibodies (R&D) together with a chemiluminescent substrate (Immun-Star Western C Kit, Biorad).

### Epitope Mapping

Epitope mapping of antibodies was performed on high-density peptide arrays as previously described,<sup>24</sup> where each array contained 12-mer peptides with 11-residue overlap to the next peptide, thereby covering the regions of the protein fragments used for antibody generation.

### Data Analysis

**Data Processing.** The data analysis was performed in the statistical computing software R.<sup>25</sup> Data sets from the initial untargeted screening and the targeted discovery, both generated with 384-plex assays, were preprocessed in the following steps: sample outliers were detected by robust principal component analysis (rPCA) using the “rrcov” R package, and for these samples, all MFI values for the outliers were removed.<sup>26</sup> The refined data were subjected to probabilistic quotient normalization (PQN),<sup>27</sup> followed by plate normalization, which for each antibody intensity profile adjusts the mean of each plate toward the mean of all plates by the local average of other antibodies.<sup>28</sup> For verification of protein profiles in plasma, the data generated by the 101-plex bead array on two 384-well plates (denoted plates #1 and #2) were subjected to outlier removal and PQN normalization, as previously described. Plates #1 and #2, with a similar distribution of samples per patient group, were normalized independently and treated as two separate data sets. Out of 579 patient samples, 443 were used for statistical analysis (Table 1B) after carefully excluding samples classified as outliers ( $N = 13$ ), samples from a compromised delivery ( $N = 118$ ), and PPMS samples ( $N = 5$ ). The data sets were further processed by a linear regression normalization of log-transformed data, where the MFI values for each antibody were adjusted by four covariates: shipment, labeling plate, age, and gender. The gender covariate was added to the intensity ≈ shipment + plate + age normalization only if it significantly (Anova  $P$  value <0.05) contributed to the model. The data set obtained for verification of IRF8 in plasma was not processed prior statistical analysis due to the small number of samples analyzed. For the

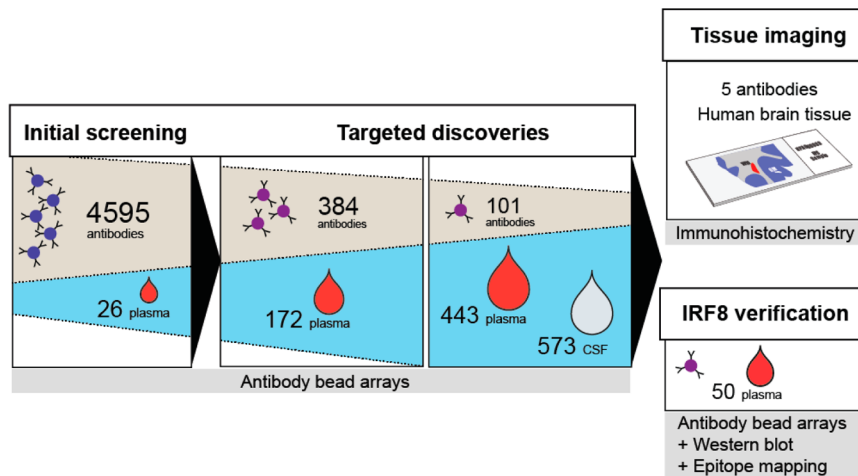


**Figure 1.** Study overview. Over initial screening and targeted discovery analysis, protein profiles were generated in plasma from more than 170 000 immunoassays on antibody suspension bead arrays. In the screening phase, 3450 unique proteins targeted by 4595 antibodies were profiled for untargeted discovery in 22 plasma samples from MS cases and nondiseased controls. 384 antibodies toward 334 proteins, including 48 proteins that had been selected from the initial screening, were then used for a targeted discovery in plasma from a total of 172 different individuals diagnosed with MS, CIS, or OND. To confirm initial findings, we evaluated 43 protein targets in additional sample material on a 101-plex focused bead array. A set of 443 plasma samples—out of which 124 had been included in the prior stage—and 573 CSF samples were analyzed. These body fluid profiling efforts resulted in candidate targets that were subsequently evaluated by immunofluorescence analysis of post-mortem brain tissue sections from MS patients. One of these candidate antibodies, anti-IRF8, was further verified in an independent set of 50 plasma samples and characterized by Western blot analysis and epitope mapping.

data obtained from CSF analysis using the 101-plex bead array, PQN normalization was performed, and in total 28 sample outliers were removed by rPCA.

**Statistical Analysis.** All  $p$  values from two-group comparisons were generated by Mann–Whitney tests using log-transformed data. If stated,  $p$  values were adjusted for multiple testing by Bonferroni correction. Lasso logistic regression implemented in the “penalized” R-package<sup>29,30</sup> was applied to build a multivariate classification model for two patient groups. The tuning parameter lambda for the pairwise classifier was determined by five-fold cross-validation, and the optimal lambda was chosen to have maximum cross-validated likelihood.<sup>30</sup> Because during cross-validation each random separation of the data into subsets gives rise to a variation of the optimal value, the cross-validations with dissimilar splits were repeated 100 times to obtain a stable parameter. The Lasso model was fitted with the mean of 100 lambdas to all data in plate #1 from the plasma verification phase. Then, the classification accuracy was assessed using the data from the separate set of samples in plate #2. The selection of contributing variables in the resulting antibody panel was performed simultaneously by Lasso. Variation in the data was assessed for plate #1 and plate #2 by the percentage of coefficients of variation (% CV), which was calculated as the average % CV across all antibody profiles in 16 replicates of a pooled sample. For correlation network analysis in plasma and in CSF, the data were log-transformed, mean-centered, and scaled before combining both plates. Correlation was calculated using Spearman rank correlation coefficients ( $\rho$ ) in separate correlation matrices for the different patient groups.  $\rho$  values, both in plasma and CSF, were further visualized in correlation network diagrams<sup>31</sup> using Cytoscape.<sup>32</sup> This data set was also used for unsupervised hierarchical clustering (Euclidian distances) of SPMS and CIS samples and a direct plasma-CSF correlation for paired samples. Jalview software<sup>33</sup> was used for sequence alignment and tree construction of peptide sequences revealed by epitope mapping; for all peptide

sequences with signals over local background  $>3$ , multiple sequence alignments were performed by ClustalO and BLOSUM62 was used for tree construction. The logos were created using WebLogo,<sup>34</sup> and a similarity search was performed using the NCBI BLASTP (ver. 2.2.29) algorithm and scored with PAM30 matrices.

#### Tissue Analysis

**Immunofluorescence.** Multiple immunofluorescence immunohistochemistry was performed on 7  $\mu\text{m}$  thick human cortex sections containing chronic and acute lesions cut from paraffin-embedded blocks on a sliding microtome and mounted onto glass slides coated with 3-aminopropyltriethoxysilane (Sigma). Sections containing human cortex cores ( $\phi$  2 mm) from individuals without clinical signs of neuropsychiatric disease part served as controls. All sections were stained on an automated Leica Bond RX system. Briefly, sections were deparaffinized (Bond Dewax solution AR9222), rehydrated, and treated for 40 min in an EDTA-based pH 9.0 solution (Bond Epitope Retrieval solution 2 AR9640) to unmask the antigens. Slides were then incubated in normal donkey serum for 30 min, followed by the addition of the primary antibody cocktail mix (containing IBA-1 and one HPA antibody) diluted in Bond Primary antibody diluent (AR9352) for 8 h at room temperature. Sections were washed 3  $\times$  15 min in PBS and incubated for 90 min at room temperature with secondary antibody cocktail mix (Cy3-labelled anti-rabbit and Cy5-labelled anti-goat) diluted 1/200 in 0.2 M PB. Sections were washed 3  $\times$  15 min in PBS and subsequently incubated for 8 h with 488-conjugated mouse anti-GFAP antibody (diluted in Bond Primary antibody diluent) at room temperature. Slides were washed 3  $\times$  15 min in PBS and counterstained with Hoechst 33342 (diluted 1:10 000 in PBS) for 30 min at room temperature. Finally, slides were incubated for 30 min in 1% Sudan Black solution in 70% ethanol to quench autofluorescence and mounted in PVA-DABCO.

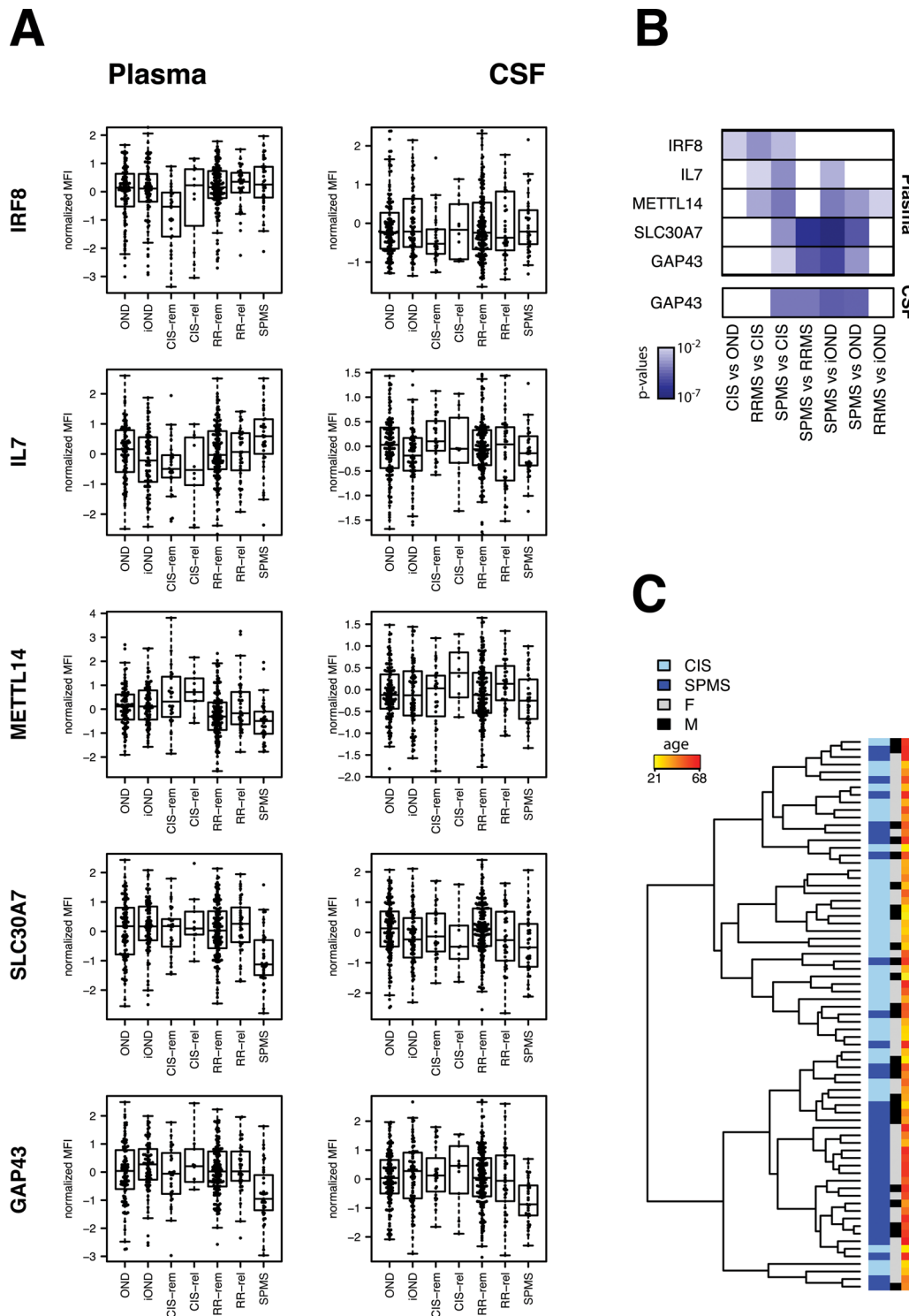


**Figure 2.** Candidate protein profiles in plasma and CSF. (A) Antibodies targeting IRF8, IL7, METTL14, SLC30A7, and GAP43 revealed differential levels in plasma from 443 individuals (left panel). For the same antibodies, corresponding plots are shown for 573 CSF individuals (right panel), with 418 individuals overlapping between plasma and CSF. Data shown are both normalized and scaled. For visualization purposes, outliers are not shown. (B) Overview of two-group comparisons performed between the main MS subtypes, for each of the five proteins and on both plasma and CSF. (C) Unsupervised hierarchical cluster analysis for CIS and SPMS plasma using the five antibodies resulted in two main clusters, each being enriched for either of the two subtypes. No gender-related enrichment was observed, and by definition, SPMS patients were older than those of CIS. The corresponding plot for CSF can be found as Supplementary Figure 5 in the Supporting Information.

**Slide Scanning Microscopy.** Fluorescence microscope images were acquired on a Vslide slide scanning microscope (MetaSystems, Altlussheim, Germany) equipped with a CoolCube 1 camera (12 bit gray scale), 10 $\times$  and 20 $\times$

objectives and filter sets for DAPI (EX350/S0 - EM470/40), FITC (EX493/16 – EMS27/30), Cy3 (EX546/10 – EMS80/30), Cy3.5 (EX581/10 – EM617/40), and Cy5 (EX630/20–647/long pass). Whole microscope slides were scanned at 2.5  $\times$

**Table 2. Multivariate Analysis<sup>a</sup>**

comparison	AUC	gene names	ENSG ID	antibodies
RRMS vs CIS	0.72	IRF8	ENSG00000140968	HPA002531
		METTL14	ENSG00000145388	HPA038001
CIS vs SPMS	0.80	ANXA1	ENSG00000135046	HPA011271
		IL7	ENSG00000104432	HPA019590
OND vs SPMS	0.78	IRF8	ENSG00000140968	HPA002531
		METTL14	ENSG00000145388	HPA038001
RRMS vs SPMS	0.77	TJP2	ENSG00000119139	HPA001813
		ALPK2	ENSG00000198796	HPA029801
OND vs SPMS	0.78	ANXA1	ENSG00000135046	HPA011271
		APEX1	ENSG00000100823	HPA002564
RRMS vs SPMS	0.77	DNMT3B	ENSG00000088305	HPA001595
		IL7	ENSG00000104432	HPA019590
OND vs SPMS	0.78	IRF8	ENSG00000140968	HPA002531
		SLC30A7	ENSG00000162695	HPA018034
RRMS vs SPMS	0.77	TJP2	ENSG00000119139	HPA001813
		ZFP36L1	ENSG00000185650	HPA035423
OND vs SPMS	0.78	ALPK2	ENSG00000198796	HPA029801
		ANXA1	ENSG00000135046	HPA011271
RRMS vs SPMS	0.77	DNMT3B	ENSG00000088305	HPA001595
		IL7	ENSG00000104432	HPA019590
OND vs SPMS	0.78	SLC30A7	ENSG00000162695	HPA018034
		TJP2	ENSG00000119139	HPA001813
RRMS vs SPMS	0.77	ZFP36L1	ENSG00000185650	HPA035423

<sup>a</sup>Lasso logistic models were fitted to plate 1 data for pair-wise classifications. The performance of each model was evaluated using the data from a separate set of individuals in plate 2. Only classifiers with AUC > 0.7 are shown. Corresponding ROC curves are shown in Supplementary Figure 4 in the Supporting Information.

, and tissue was detected based on the Hoechst 33342 signal. After generating a position map, all tissue-covered areas were scanned using 20× primary objective. Individual field of view images were stitched to generate a large four-channel fluorescence image of the entire specimen with microscopic resolution. Images obtained with Vslide were analyzed using Metaviewer (Metasystems).

**Laser-Scanning Microscopy.** On the basis of the generated tissue scans, areas with clear inflammatory processes and more “healthy” appearing areas were selected for further investigation. Images were acquired on a 780LSM confocal laser-scanning microscope (Zeiss). Emission spectra for each dye were limited as follows: Hoechst (420–485 nm), Cy2 (505–530 nm), Cy3 (560–610 nm), and Cy5 (640–720 nm). Coexistence was defined as immunosignals being present without physical signal separation in ≤1.0 μm optical slices at 40× (Plan-Neofluar 40 × /1.30) or 63× (Plan-Apochromat 63 × /1.40) primary magnification. Images obtained with the Zeiss confocal microscope were analyzed using the ZEN software package (Zeiss).

## RESULTS

Here we employed an affinity proteomics approach to identify proteins related to MS by using antibodies on three different types of sample material: plasma, CSF, and brain tissue. Starting with multiplexed antibody suspension bead arrays, protein profiles were generated in three sets of plasma samples as well as in partially paired CSF samples. Lastly, the interesting antibodies were chosen to stain sections from MS brain tissues (Figure 1).

### Initial Discovery Screening

Protein profiles were generated from plasma with 4595 HPA antibodies targeting 3450 unique proteins in 12 rounds of

analysis on 384-plex bead arrays. Plasma from 16 MS patients (8 RRMS, 4 SPMS, 4 PPMS) and 6 nondiseased controls was analyzed, alongside 760 other serum and plasma samples within cancer, cardiovascular, and neurodegenerative diseases (data not shown). Antibodies that revealed profiles of significant differences ( $p < 0.05$ ) between the 16 MS cases and 6 nondiseased controls were evaluated for further investigations. These were selected if they were (i) MS-specific in comparison with the other profiled neurodegenerative diseases or (ii) of potential relevance according to the biological processes related to a specific target. This investigation resulted in a refined list of 56 antibodies against 48 target proteins (Supplementary Table 2A in the Supporting Information), including one of the highlighted targets of the herein presented study, methyltransferase-like protein 14 (METTL14).

### First Targeted Discovery Across MS Subtypes

Following the previously described initial discovery analysis based on 3450 targets, 296 additional protein targets were selected based on a thorough and inclusive literature search, including proteomic studies in blood or CSF,<sup>35–42</sup> a genome wide association study,<sup>43</sup> blood transcriptome analysis,<sup>44</sup> and other related works<sup>10,23,41,45–54</sup> as well as previous results from internal neuroscience related protein profiling efforts. Subsequently, this first targeted 384-plex bead array for 334 proteins was created to profile an additional set of 172 plasma samples (Table 1). The SPMS-CIS (CIS-rel and CIS-rem combined) comparison revealed elevated protein profiles in SPMS for interleukin 7 (IL7, HPA019590; adjusted  $p = 0.001$ ) and S100 calcium binding protein A8 (S100A8, HPA024372; adjusted  $p = 0.02$ ). Similar differences with these two protein profiles were also found when comparing RRMS (RR-rel and RR-rem combined)-CIS (adjusted  $p = 0.03$ ). An antibody targeting myotrophin (MTPN, HPA019735), showed higher

intensities in the SPMS subtype compared with CIS (adjusted  $p = 0.01$ ). Additional SPMS-CIS differences were revealed for interferon regulatory factor 8 (IRF8, HPA002531;  $p = 0.03$ ) and serine proteinase inhibitor member 3 (SERPINA3, HPA002560;  $p = 0.009$ ), when  $p$  values were not adjusted for multiple testing. For follow-up experiments, these tentative candidates as well as antibodies generated against different epitopes of the same proteins were included.

### Second Targeted Analysis Across MS Subtypes

A second focused bead array was built on the above indications and by adding antibodies from a previous CSF profiling study.<sup>23</sup> This list was again supplemented with other internally identified targets from screening an independent MS-related serum sample cohort (data not shown). The resulting 101-plex bead array addressed 43 proteins (Supplementary Table 2B in the Supporting Information), and was used to analyze an extended set of 443 plasma samples from patients with OND, iOND, CIS, RRMS, and SPMS (Table 1B). Here assays were performed in two separate 384-well plates with %CV of 6.5 for plate #1 and 5.1 for plate #2.

In concordance with the findings above, two-group univariate comparisons revealed most significant differences between SPMS-CIS groups (Figure 2A,B, Supplementary Table 4 in the Supporting Information) and by antibodies against IL7, IRF8, METTL14, the zinc transporter solute carrier family 30 member 7 (SLC30A7), as well as the growth associated protein 43 (GAP43). For these five candidates, we observed no gender effects ( $p > 0.05$ ) but an interindividual spread in MFI values within each subtype and even prior normalization (Supplementary Figure 1 in the Supporting Information). Statistically significant differences ( $p < 0.05$ ) were reproducible (Supplementary Figure 2 in the Supporting Information); as an example, anti-IRF8 HPA002531 showed a high correlation (plate1: spearman  $Rho = 0.91$ ; plate2:  $Rho = 0.89$ ) when this antibody was utilized in a different bead array composition on the very same set of samples. These SPMS-CIS differences were further illustrated by unsupervised hierarchical clustering of plasma protein profiles for these two patient groups (Figure 2C). Models for multiparameter comparison across disease subtypes were then calculated using Lasso logistic regression and summarized in Table 2 and Supplementary Figure 3 in the Supporting Information; area under the curve (AUC) values of up to 0.80 could be achieved with antibody panels consisting of varying number of antibodies. An IRF8 contribution was found for all but the RRMS-SPMS comparison.

### Verification Analysis for IRF8

For further evaluation of differences between SPMS, CIS, and RRMS, an independent set of plasma samples was analyzed (Table 1D), where RRMS and CIS subtypes were age- and gender-matched, while diagnosis of SPMS is inherently related to older age. In contrast with previous analysis, METTL14, SLC30A7, IL7, and GAP43 did not reveal statistically significant differences (data not shown), and there was a significant difference for IRF8 (HPA002531) between genders ( $p = 0.02$ ). But as shown in Figure 3, a separate analysis using the 37 female patients revealed elevated IRF8 levels for SPMS compared with CIS ( $p = 0.001$ ) and RRMS ( $p = 0.0005$ ).

These indications lead to focus on IRF8 as the main target of interest. Three available antibodies against IRF8 were analyzed in Western blot using a cell lysate overexpressing this regulatory factor. This revealed a single band at the predicted 50 kDa range detected by all three antibodies. When analyzing a pool

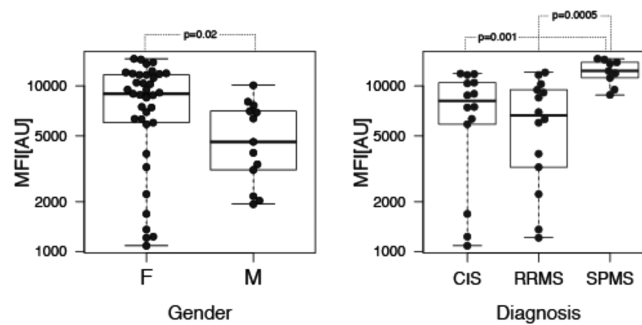


**Figure 3.** Analysis of IRF8 in an independent set of plasma samples. Signal intensities from HPA002531 (IRF8) in 50 plasma samples (CIS, RRMS (RR-rem), and SPMS). Although the signal intensities differed between males and females (left), a comparison only within the 37 female individuals revealed statistically significant and elevated signal intensities in SPMS samples compared with RRMS and CIS samples.

of plasma samples, only HPA002531 showed a single band at a slightly lower molecular mass of  $\pm 40$  kDa (Supplementary Figure 4A in the Supporting Information). In addition, epitope mapping was performed on high-density peptide arrays for HPA002531 on peptides covering the protein fragment that had been selected to generate this antibody. Two epitopes with consensus peptide sequences, PYKVYRIVPEE and MEIAEV-DSVVPVNN, were found (Supplementary Figure 4B in the Supporting Information). A homology search for the first consensus sequence revealed 100% similarity to the 106–116 amino acid region of IRF8 ( $E$  value =  $1 \times 10^{-5}$ ), whereas the second consensus sequence showed a nonsignificant similarity of 64% to the predicted human protein GA-binding protein subunit beta-2 isoform X6 (GABPB2,  $E$  value = 1.3).

### Profiling of Paired CSF Samples

The targeted 101-plex bead array was then used to analyze a set of 573 CSF samples (Table 1C). As previously reported,<sup>23</sup> a subset of these CSF samples ( $n = 339$ ) had been analyzed and revealed that levels for GAP43 and SERPINA3 were altered between MS subtypes and controls. The current analysis with 573 samples shown in Figure 2A (see Supplementary Figure 5A in the Supporting Information for analysis of the new 234 sample subset) confirmed these observations. GAP43 was detected at lower levels in SPMS compared with RRMS, OND, and iOND groups ( $p < 0.007$ ). Also, antibodies against SERPINA3 confirmed previous analysis and showed higher levels in RRMS and iOND groups ( $p < 0.001$ , Supplementary Figure 5A in the Supporting Information). For both targets, profiles obtained by paired antibodies revealed correlating intensities (Supplementary Figure 5B in the Supporting Information). Apart from GAP43, protein profiles determined in CSF did not confirm indications found in plasma (Figure 2B). A correlation analysis between paired plasma and CSF samples did not reveal congruence in protein profiles with  $-0.5 < Rho < 0.5$  (data not shown).

### Correlation Networks Across MS Subtypes

In the second targeted analysis phase, we also studied differential correlation of protein profiles across MS subtypes in plasma and CSF to investigate the relation between the five highlighted protein profiles within each subtype. As shown for plasma in Figure 4, network analysis revealed a prominent positive correlation between SLC30A7 and GAP43 in all subtypes. Also, a higher correlation between IL7 and IRF8

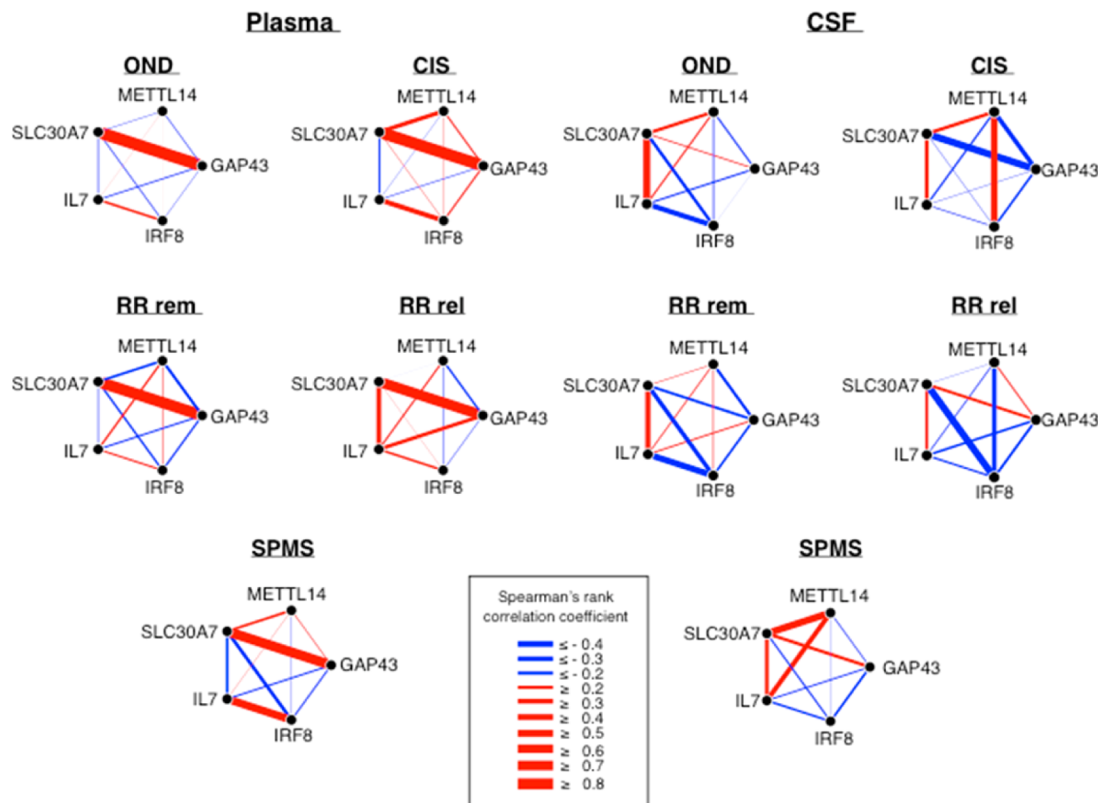


**Figure 4.** Correlation networks of candidate profiles in plasma and CSF. Network diagrams were generated to summarize correlation relationships between the five highlighted proteins for subtypes of MS and OND and both plasma (left panel) and CSF (right panel). For all combinations of these five proteins, Spearman's rank correlation coefficient was calculated between MFI values for any given two proteins within each sample group and sample type, and the correlations were visualized in the network diagrams. The strength and direction of correlation coefficients were visualized with different line widths and colors. The network diagrams demonstrate considerable differences in correlation relations across these five proteins within plasma and CSF. Note, for example, the strong positive correlation between SLC30A7 and GAP43 exclusively unveiled in plasma samples of all sample groups. Furthermore, two correlation relations were uniquely revealed for the SPMS subgroup: the positive correlations between IL7 and IRF8 in plasma and IL7 and METTL14 in CSF.

**Table 3. Annotation of Candidate Expression in Brain Tissue<sup>a</sup>**

location	antibody	gene name	annotation
neuronal	HPA015600	GAP43	MS: intense axon-like staining pattern normal: N/A
	HPA019590	IL7	MS: moderate to strong expression in neurons (soma and processes) and some blood vessels normal: weak to moderate in perikarya
	HPA002531	IRF8	MS: strong staining in perikarya (including axonal processes) and blood vessels normal: moderate staining in neuronal perikarya
	HPA038001	METTL14	MS: moderate to strong staining in neurons (mainly nuclear and some processes and some inflammatory cells) Normal: moderate to strong expression, mostly nuclear
glial	HPA018034	SLC30A7	MS: moderate immunoreactivity in blood vessels and microglia normal: N/A
	HPA024372	S100A8	MS: strong expression in macrophages and some blood vessels normal: no expression detected
endothelial	HPA000893	SERPINA3	MS: almost exclusively expressed in blood vessels normal: no expression detected

<sup>a</sup>Summary of the staining pattern observed for candidate markers on normal and MS brain tissue.

profiles was found in SPMS compared with other groups. In CSF, however, a positive correlation between SLC30A7 and IL7 was observed in all subtypes. Notably, profiles for IL7 and METTL14 were most similar in SPMS, while METTL14 was concordant with IRF8 in CIS, however, discordant in relapsing RRMS. Thus, indications for subtype specific networks were

shown, and intranetwork relations were found to be dependent on the type of the analyzed body fluid.

#### Distribution of Identified Targets in the MS Brain

Following the analysis of body fluid samples, antibodies identified for IRF8, METTL14, IL7, GAP43, SERPINA3, and SLC30A7 were applied to brain tissue sections from MS patients (Table 3 and Supplementary Table 1 in the Supporting

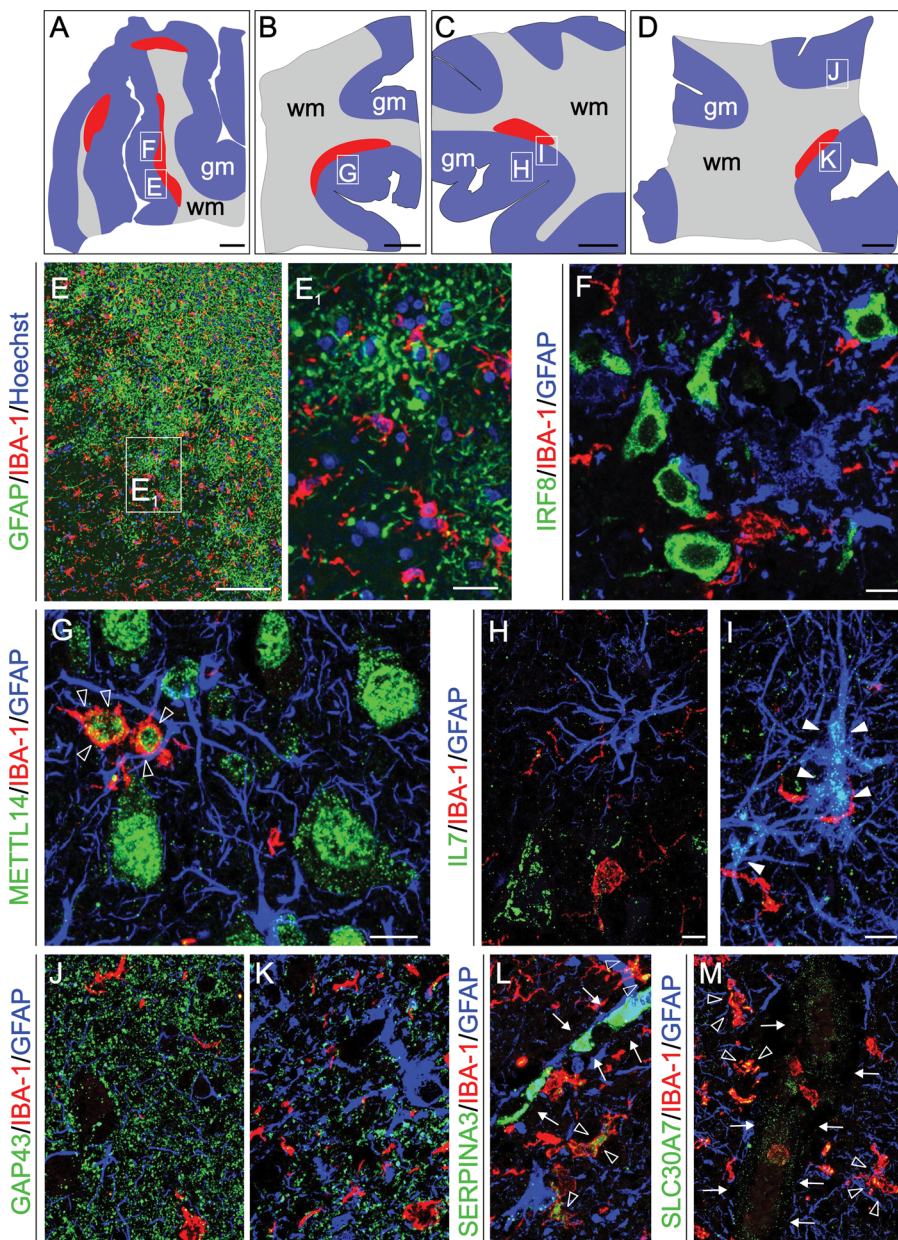


**Figure 5.** Expression of candidate proteins in human MS brain tissue. Selected antibodies were applied to three to four cortical brain sections containing a single or multiple lesions. (A–D) Schematic drawing of the specimens illustrating gray (blue color) and white matter (light gray color) structures and identified lesion sites (red color). (E) All specimens were stained with antibodies against the astrocyte marker GFAP and microglia marker IBA1 in combination with antibodies directed against the selected targets. Panel E shows the distribution of GFAP and IBA1-immunoreactivity at the border of a plaque. The presence of numerous IBA1-immunoreactive microglia indicates that this is an active lesion (E<sub>1</sub>). (F) IRF8-immunoreactivity could only be detected in neuron-like cells throughout the examined brain sections including the gray matter near lesions. (G) Neuron-like mainly nuclear staining pattern was observed for METTL14. In addition, a nuclear staining in microglia (open arrowheads in G) could also be identified. (H) IL7-immunoreactivity was limited to sparsely distributed neuron-like cells and (I) GFAP<sup>+</sup> astrocytes in MS affected areas. (J) Differences in GAP43-immunoreactivity within a single section could be observed. In areas lacking signs of sclerosis, GAP43-immunoreactivity revealed a network of fibers with strongest intensity in the deeper cortical layers. (K) In lesion sites characterized by the strong activation of astrocytes and expression of GFAP, the amount of GAP43 immunoreactivity fibers was markedly reduced. (L,M) Immunohistochemistry for SERPINA3 (L) and SLC30A7 (M) revealed labeling of IBA1<sup>+</sup> microglia for both (open arrowheads in L and M) while immunoreactivity could also be detected in the lumen of brain capillaries (arrows in L and M). Scale bars: 1 cm (A–D), 100  $\mu$ m (E), 20  $\mu$ m (E<sub>1</sub>J–M), 10  $\mu$ m (F–I).

Information). A multiplex fluorescence approach was used to investigate the expression and distribution of the MS associated proteins in the vicinity of lesions and to identify the cellular distribution of selected targets in glia cells either by expression or phagocytosis. For tissue staining, the identified antibodies were combined with antibodies for the astrocyte marker glial

fibrillary acidic protein (GFAP) and the microglia marker ionized calcium adapter molecule 1 (IBA1). On the basis of GFAP immunoreactivity and Sudan Black counterstaining, single or multiple lesions could be identified. The majority of lesions were localized at the border between gray and white matter expanding into the latter (Figure 5A–D). Most plaques

were active lesions characterized by large numbers of microglia cells within and surrounding the plaque (Figure 5E).

All selected antibodies revealed reactivity in the MS brain. IRF8 antibody HPA002531 (Figure 5F) prominently stained the majority of neurons in the proximity of lesions but also in distal healthy appearing areas of the examined brain section. The anti-IRF8 immunoreactivity was restricted to the cytosolic compartment of neurons, and no clear coexistence of IRF8 with the glial markers GFAP and IBA-1 could be observed. For METTL14, a second antibody (HPA038002) was used and revealed a cytosolic and nuclear staining pattern in neuron-like cells (Figure 5G) from both lesion affected and more healthy appearing areas. This antibody also showed reactivity in IBA1<sup>+</sup> microglia, but in these cells, METTL14 immune-reactivity was mainly nuclear. The IL7 antibody HPA019590 revealed weak to moderate staining of a few neuron-like cells in the proximity of lesions (Figure 5H) and a subset of GFAP<sup>+</sup> cells in sclerotic areas (Figure 5I). Antibody HPA015600 targeting GAP43 revealed an axon-like staining pattern with highest staining intensity in the multiform layer of the cortex (Figure 5J). A clear decrease in anti-GAP43 immunoreactivity near plaques compared with less affected areas in the same sample could be observed (Figure 5K). SERPINA3 immunoreactivity was mainly found in the lumen of smaller and larger blood vessels (HPA000893, Figure 5L) and moderate immunoreactivity could be observed in IBA1<sup>+</sup> microglia cells. No clear difference in staining intensity between plaques and more healthy appearing areas could be identified. Antibody HPA018034 recognizing the zinc transporter SLC30A7 revealed a weak immunoreactivity in the lumen of blood vessels and labeled IBA1<sup>+</sup> microglia (Figure 5M).

These findings show that possible sources of the identified targets in blood plasma and CSF were neurons (IRF8, METTL14, IL7, and GAP43) and glia cells (IL7, METTL14) in the vicinity of lesions. This supports the hypothesis that proteins expressed in the brain can leak or be transported by macrophages into the bloodstream and can effectively be detected in plasma samples. SERPINA3 and SLC30A7 were mainly located in the lumen of blood vessels, indicating that these proteins can be involved in a peripheral component of the MS pathology.

## ■ DISCUSSION

In this study, we have employed an affinity proteomics approach to profile proteins in the context of MS. Starting with unbiased assays on multiplexed antibody suspension bead arrays, a large number of antibodies were utilized to identify MS-subtype-related proteins in plasma. We then built two, subsequently smaller targeted arrays for analysis of an extended study of MS sample sets using both plasma and CSF. From these investigations, antibodies targeting IRF8, IL7, SLC30A7, METTL14, and GAP43 were most indicative for disease state and progression and consequently chosen for immunofluorescence analysis of post-mortem brain tissue sections from MS patients.

Affinity proteomics is an alternative to mass spectrometry with a conceptual difference because target selection is usually conducted prior analysis. Thus, many affinity-based approaches are hypothesis-driven and generally do not incorporate large numbers of antibodies for discovery purposes. In our initial discovery screening, antibodies were included without considering any protein-disease relation, and were selected for further analysis if they revealed differential protein profiles only

between the MS cases and controls and not in the sample sets belonging to other neurodegenerative diseases. This highlighted the profile for METTL14, which was subsequently confirmed to be differential between the CIS and SPMS groups. We further made use of the flexibility of the chosen bead array methodology and supplemented the first indications with targets suggested by literature. Profiling additional plasma samples as well as CSF samples led to a short list of candidate antibody targets, which we finally analyzed in rare brain tissue from diseased individuals as well as from non-MS individuals. While information about potential disease relation was available for IRF8, GAP43, SLC30A7, and IL7, little is known about the function of METTL14 and its potential relation to MS pathogenesis. As previously indicated,<sup>55</sup> a disease-centric selection of antibodies provides more candidates than untargeted discovery; however, they hold the potential of extending the existing knowledge.

Multiple sclerosis is widely considered to be a heterogeneous disease, indicating that further subclassification and staging might be required to better understand the differential pathophysiology. At this point, we cannot propose a novel biomarker or signature that now allows us to better classify MS, but we have shown by multivariate, as well as network analysis, that the five highlighted proteins in plasma may serve as a good basis to extend the current understanding of the disease, yet far more samples (thousands) and dedicated assays may be required to confirm that the indications we present here are valid for samples from different collections, clinics, nations, and ethnicities. It is further suggested to follow-up on or include some of the proposed candidates in coming analysis of biobanks and consider the use of multiplexed methods for multiparallel determination of MS-related proteins. An intrinsic challenge will remain in finding markers for this disease because individuals diagnosed with SPMS are generally older than those suffering from other subtypes of MS. In part, this means that associations found for a subtype may also be driven by age, gender, or other variables than disease and need to be taken into account during the statistical evaluation.

We have recently developed assays for CSF analysis on the bead array platform, which we utilized for protein profiling<sup>23</sup> as well as for autoantibody profiling.<sup>56</sup> In the presented work, basically no correlation of protein levels between paired plasma and CSF samples could be shown, which might be related to where (organ proximity) and when (related to event) the sample had been taken. For the studied MS subtypes, correlation networks based on the highlighted proteins were different in plasma compared with CSF. Such discrepancy may though be explained by the complexity of the samples as well as changes in target abundance and resulting analytical sensitivity. We found GAP43 to reveal statistically significant differences for both plasma and CSF. However, when comparing gene expression of all selected targets (Supplementary Table 5 in the Supporting Information) in different organs and tissue types,<sup>57</sup> GAP43 has 25 times higher expression in the brain compared with all other analyzed tissues. Interestingly, all other targets suggested as potential markers in plasma but not in CSF were highly expressed in multiple peripheral organs and tissue types. Even though the presence of target proteins in brain was confirmed, this suggests that a majority of target proteins detected in body fluids could originate from other tissues or appear as a consequence of an immune response. An alternative explanation for absence of targets detected in plasma but not in CSF might come from the direct interaction of (juxtapascular)

microglia with the bloodstream, as found for METTL14, SERPINA3, and SLC30A7 in IBA1+ microglia (Figure 5G,L,M).

There is still a great need for noninvasive tools to diagnose neurological disorders and monitor disease progression and efficiency of therapeutic intervention. Physiological readouts, neuroimaging, and analysis of CSF and plasma are the only acceptable diagnostic tools available to neurologists. Technological advances now enable us to use small sample quantities to detect target proteins at concentrations as low as in the range of high pg/mL in multiplex, thus making it possible to detect proteins expressed by brain cells in CSF or plasma. As indicated in this study, the challenging aspect of such an approach is to understand the relations between altered protein levels in systemic or proximal body fluids and the ongoing pathological processes in the brain. Future approaches might benefit from focusing on genes highly expressed or enriched in certain (diseased) areas of the brain or as compared with peripheral organs. As shown for GAP43 and degeneration of neurons, proteins present within these neurons can be detectable in CSF and plasma, and it would be interesting to see if other cell-type-specific proteins could also be detected in both body fluids.

Among the candidates and besides the aforementioned GAP43, we obtained most supportive evidence for antibody-based detection of IRF8. It is a transcription factor with a known function in interferon signaling, response to infection, and for the development of microphages and other myeloid lineages.<sup>58,59</sup> Alleles in the vicinity of the IRF8 gene have been associated with MS susceptibility,<sup>60,61</sup> suggesting that disease susceptibility is potentially linked to the regulation of IRF8 transcription. Moreover, a very recent study in mouse models and neuroinflammation showed that *IRF8*<sup>-/-</sup> mice were resistant to experimental autoimmune encephalomyelitis and that expression of IRF8 in antigen-presenting cells facilitated disease onset and progression.<sup>62</sup> We, for instance, found that profiles from IL7 and IRF8 were similar in SPMS plasma but not in CSF, and the antibody reactivity in tissue was located to the majority of neurons close to lesions. Still, more insights need to be obtained to further define the role of IRF8 in disease development, but our study shows that using affinity proteomics tools across different samples types and analytical assays may contribute to that aim. Regarding IL7, we recently obtained elevated levels in plasma from the IL7 antibody HPA019590 when studying childhood malaria,<sup>55</sup> and as shown elsewhere, levels of IL7 were increased in relation to RRMS.<sup>63</sup> Less is known about METTL14, which was newly linked to methylation of nuclear RNA,<sup>64</sup> as well as about the zinc transporter SLC30A7.

In summary, integrative affinity proteomic approaches were used for analysis of plasma, CSF and brain tissue to identify candidate proteins, in particular, IRF8, for further investigations. We demonstrated the broad-scale applicability of antibodies across different samples types and platforms and indicate that the use of multiplexed affinity-proteomics methods holds a promise for identification of proteins, which can be investigated further for an improved understanding of molecular mechanism of neurological diseases such as MS. Further studies across different biobanks are now needed to determine the contribution of our findings to a better understanding of the MS and its subtypes.

## ASSOCIATED CONTENT

### S Supporting Information

S-Table 1: Demographics of brain tissue samples. S-Table 2A: Antibodies suggested by discovery screening. S-Table 2B: Antibodies used for second, focused 101-plex bead array. S-Table 3: Antibody performance in plasma and CSF. S-Table 4: Antibodies used for analysis of brain tissue. S-Table 5: RNA expression levels (FPKM) related to candidate proteins. S-Figure 1: Protein profiles prior normalization. S-Figure 2: Experimental reproducibility of candidate profiles. S-Figure 3: ROC curves from multivariate analysis. S-Figure 4: Western blot and epitope mapping of IRF8. S-Figure 5: Candidate profiles in CSF. S-Figure 6: Hierarchical clustering of SPMS and CIS in CSF. This material is available free of charge via the Internet at <http://pubs.acs.org>.

## AUTHOR INFORMATION

### Corresponding Author

\*E-mail: jochen.schwenk@scilifelab.se. Tel: +46 (0)8 5248 1482.

### Author Contributions

<sup>†</sup>S.B. and B.A. contributed equally.

### Notes

The authors declare no competing financial interest.

## ACKNOWLEDGMENTS

We thank the whole group of Biobank Profiling-Affinity Proteomics at SciLifeLab Stockholm and the entire staff of the Human Protein Atlas for their efforts in generating the antibodies. We also thank the clinical teams and biobank staff who helped with sample collection. We thank Hjalmar Brismar and Hans Blom at SciLifeLab for providing access to microscopes. This work was supported by grants from the Swedish Research Council, the Swedish Brain Foundation, the AFA Foundation, as well as SciLifeLab and the Knut and Alice Wallenberg Foundation.

## ABBREVIATIONS

AUC, area under curve; CIS, clinically isolated syndrome; CSF, cerebrospinal fluid; CV, coefficient of variation; GAP43, growth associated protein 43; GFAP, glial fibrillary acidic protein; HPA, Human Protein Atlas; IBA1, ionized calcium adapter molecule 1; IL7, interleukin 7; IRF8, interferon regulatory factor 8; METTL14, methyltransferase-like protein 14; MFI, median fluorescence intensity; MS, multiple sclerosis; OND, other neurological diseases; iOND, OND with signs of inflammation; PCA, principal component analysis; PPMS, primary progressive MS; PrEST, protein epitope signature tag; PQN, probabilistic quotient normalization; ROC, receiver operating characteristics; RRMS, relapsing remitting MS; SLC30A7, zinc transporter solute carrier family 30 member 7; SPMS, secondary progressive MS

## REFERENCES

- (1) Karussis, D. The diagnosis of multiple sclerosis and the various related demyelinating syndromes: a critical review. *J. Autoimmun.* **2014**, *48–49*, 134–142.
- (2) Milo, R.; Miller, A. Revised diagnostic criteria of multiple sclerosis. *Autoimmun. Rev.* **2014**, *13* (4–5), 518–524.

- (3) Leary, S. M.; Porter, B.; Thompson, A. J. Multiple sclerosis: diagnosis and the management of acute relapses. *Postgrad. Med. J.* **2005**, *81* (955), 302–308.
- (4) Keegan, B. M.; Noseworthy, J. H. Multiple sclerosis. *Annu. Rev. Med.* **2002**, *53*, 285–302.
- (5) Polman, C. H.; et al. Diagnostic criteria for multiple sclerosis: 2010 revisions to the McDonald criteria. *Ann. Neurol.* **2011**, *69* (2), 292–302.
- (6) Disanto, G.; et al. Heterogeneity in multiple sclerosis: scratching the surface of a complex disease. *Autoimmune Dis.* **2010**, *2011*, 932351.
- (7) Lucchinetti, C.; et al. Heterogeneity of multiple sclerosis lesions: implications for the pathogenesis of demyelination. *Ann. Neurol.* **2000**, *47* (6), 707–717.
- (8) Kroksveen, A. C.; et al. Proteomics of human cerebrospinal fluid: discovery and verification of biomarker candidates in neurodegenerative diseases using quantitative proteomics. *J. Proteomics* **2011**, *74* (4), 371–388.
- (9) Tumani, H.; et al. Cerebrospinal fluid biomarkers in multiple sclerosis. *Neurobiol. Dis.* **2009**, *35* (2), 117–127.
- (10) Bielekova, B.; Martin, R. Development of biomarkers in multiple sclerosis. *Brain* **2004**, *127* (Pt 7), 1463–1478.
- (11) Farias, A. S.; et al. Ten years of proteomics in multiple sclerosis. *Proteomics* **2014**, *14* (4–5), 467–480.
- (12) Comabella, M.; Montalban, X. Body fluid biomarkers in multiple sclerosis. *Lancet Neurol* **2014**, *13* (1), 113–126.
- (13) Uhlen, M.; et al. Towards a knowledge-based Human Protein Atlas. *Nat. Biotechnol.* **2010**, *28* (12), 1248–1250.
- (14) Uhlen, M.; et al. A human protein atlas for normal and cancer tissues based on antibody proteomics. *Mol. Cell. Proteomics* **2005**, *4* (12), 1920–1932.
- (15) Stoevesandt, O.; Taussig, M. J. Affinity proteomics: the role of specific binding reagents in human proteome analysis. *Expert Rev. Proteomics* **2012**, *9* (4), 401–414.
- (16) Ayoglu, B.; et al. Systematic antibody and antigen-based proteomic profiling with microarrays. *Expert Rev. Mol. Diagn.* **2011**, *11* (2), 219–234.
- (17) McDonald, W. I.; et al. Recommended diagnostic criteria for multiple sclerosis: guidelines from the International Panel on the diagnosis of multiple sclerosis. *Ann. Neurol.* **2001**, *50* (1), 121–127.
- (18) De Groot, C. J.; et al. Post-mortem MRI-guided sampling of multiple sclerosis brain lesions: increased yield of active demyelinating and (p)reactive lesions. *Brain* **2001**, *124* (Pt 8), 1635–1645.
- (19) Kampf, C.; et al. Production of tissue microarrays, immunohistochemistry staining and digitalization within the human protein atlas. *J. Vis. Exp.* **2012**, No. 63, 3620.
- (20) Nilsson, P.; et al. Towards a human proteome atlas: high-throughput generation of mono-specific antibodies for tissue profiling. *Proteomics* **2005**, *5* (17), 4327–4337.
- (21) Sjoberg, R.; et al. Validation of affinity reagents using antigen microarrays. *New Biotechnol.* **2012**, *29* (5), 555–563.
- (22) Drobin, K.; Nilsson, P.; Schwenk, J. M. Highly multiplexed antibody suspension bead arrays for plasma protein profiling. *Methods Mol. Biol.* **2013**, *1023*, 137–145.
- (23) Haggmark, A.; et al. Antibody-based profiling of cerebrospinal fluid within multiple sclerosis. *Proteomics* **2013**, *13* (15), 2256–2267.
- (24) Forsstrom, B. Proteome-wide epitope mapping of antibodies using ultra-dense peptide arrays. *Mol. Cell. Proteomics* **2014**, *13*, 1585–1597.
- (25) Ihaka, R.; Gentleman, R. R: a language for data analysis and graphics. *J. Comput. Graphical Statistics* **1996**, *5*, 299–3214.
- (26) Hubert, M.; Rousseeuw, P. J.; Branden, K. V. ROBPCA: A new approach to robust principal component analysis. *Technometrics* **2005**, *47* (1), 64–79.
- (27) Dieterle, F.; et al. Probabilistic quotient normalization as robust method to account for dilution of complex biological mixtures. Application in <sup>1</sup>H NMR metabonomics. *Anal. Chem.* **2006**, *78* (13), 4281–4290.
- (28) Hong, M.-G., et al. Multi-Dimensional Normalization of Plate Effects in the Application of Affinity Proteomics for Plasma Profiling, unpublished.
- (29) Goeman, J. J. L1 penalized estimation in the Cox proportional hazards model. *Biometrical journal. Biometrische Zeitschrift* **2010**, *52* (1), 70–84.
- (30) Tibshirani, R. Regression shrinkage and selection via the Lasso. *Journal of the Royal Statistical Society Series B-Methodological* **1996**, *58* (1), 267–288.
- (31) Britschgi, M.; et al. Modeling of pathological traits in Alzheimer's disease based on systemic extracellular signaling proteome. *Mol. Cell. Proteomics* **2011**, *10* (10), M111 008862.
- (32) Smoot, M. E.; et al. Cytoscape 2.8: new features for data integration and network visualization. *Bioinformatics* **2011**, *27* (3), 431–432.
- (33) Waterhouse, A. M.; et al. Jalview Version 2—a multiple sequence alignment editor and analysis workbench. *Bioinformatics* **2009**, *25* (9), 1189–1191.
- (34) Crooks, G. E.; et al. WebLogo: a sequence logo generator. *Genome Res.* **2004**, *14* (6), 1188–90.
- (35) Suk, K. Combined analysis of the glia secretome and the CSF proteome: neuroinflammation and novel biomarkers. *Expert Rev. Proteomics* **2010**, *7* (2), 263–274.
- (36) Stoop, M. P.; et al. Proteomics comparison of cerebrospinal fluid of relapsing remitting and primary progressive multiple sclerosis. *PLoS One* **2010**, *5* (8), e12442.
- (37) Sakurai, T.; et al. Identification of antibodies as biological markers in serum from multiple sclerosis patients by immunoproteomic approach. *J. Neuroimmunol.* **2011**, *233* (1–2), 175–180.
- (38) Ottervald, J.; et al. Multiple sclerosis: Identification and clinical evaluation of novel CSF biomarkers. *J. Proteomics* **2010**, *73* (6), 1117–1132.
- (39) Noben, J. P.; et al. Lumbar cerebrospinal fluid proteome in multiple sclerosis: characterization by ultrafiltration, liquid chromatography, and mass spectrometry. *J. Proteome Res.* **2006**, *5* (7), 1647–1657.
- (40) Hammack, B. N.; et al. Proteomic analysis of multiple sclerosis cerebrospinal fluid. *Mult. Scler.* **2004**, *10* (3), 245–260.
- (41) Alexander, J. S.; et al. Alterations in serum MMP-8, MMP-9, IL-12p40 and IL-23 in multiple sclerosis patients treated with interferon-beta1b. *Mult. Scler.* **2010**, *16* (7), 801–809.
- (42) Sawcer, S.; et al. Genetic risk and a primary role for cell-mediated immune mechanisms in multiple sclerosis. *Nature* **2011**, *476* (7359), 214–219.
- (43) Gandhi, K. S.; et al. The multiple sclerosis whole blood mRNA transcriptome and genetic associations indicate dysregulation of specific T cell pathways in pathogenesis. *Hum. Mol. Genet.* **2010**, *19* (11), 2134–2143.
- (44) Zeis, T.; et al. Normal-appearing white matter in multiple sclerosis is in a subtle balance between inflammation and neuroprotection. *Brain* **2008**, *131* (Pt 1), 288–303.
- (45) Valdo, P.; et al. Enhanced expression of NGF receptors in multiple sclerosis lesions. *J. Neurol., Neurosurg. Psychiatry* **2002**, *61* (1), 91–98.
- (46) Thangarajh, M.; et al. Increased levels of APRIL (a proliferation-inducing ligand) mRNA in multiple sclerosis. *J. Neuroimmunol.* **2005**, *167* (1–2), 210–214.
- (47) Tanaka, M.; et al. Anti-aquaporin 4 antibody in Japanese multiple sclerosis: the presence of optic spinal multiple sclerosis without long spinal cord lesions and anti-aquaporin 4 antibody. *J. Neurol., Neurosurg. Psychiatry* **2007**, *78* (9), 990–992.
- (48) Solomon, B. D.; et al. Neuropilin-1 attenuates autoreactivity in experimental autoimmune encephalomyelitis. *Proc. Natl. Acad. Sci. U. S. A.* **2011**, *108* (5), 2040–2045.
- (49) Reder, A. T. MxA: a biomarker for predicting multiple sclerosis disease activity. *Neurology* **2010**, *75* (14), 1222–1223.
- (50) Ramanathan, M.; et al. In vivo gene expression revealed by cDNA arrays: the pattern in relapsing-remitting multiple sclerosis

patients compared with normal subjects. *J. Neuroimmunol.* **2001**, *116* (2), 213–219.

(51) Mc Guire, C.; et al. Oligodendrocyte-specific FADD deletion protects mice from autoimmune-mediated demyelination. *J. Immunol.* **2010**, *185* (12), 7646–7653.

(52) Lindsey, J. W.; Agarwal, S. K.; Tan, F. K. Gene expression changes in multiple sclerosis relapse suggest activation of T and non-T cells. *Mol. Med.* **2011**, *17* (1–2), 95–102.

(53) Harris, V. K.; et al. Bri2–23 is a potential cerebrospinal fluid biomarker in multiple sclerosis. *Neurobiol. Dis.* **2010**, *40* (1), 331–339.

(54) Alcina, A.; et al. The autoimmune disease-associated KIFSA, CD226 and SH2B3 gene variants confer susceptibility for multiple sclerosis. *Genes Immun.* **2010**, *11* (5), 439–445.

(55) Bachmann, J.; et al. Affinity proteomics reveals elevated muscle proteins in plasma of children with cerebral malaria. *PLoS Pathog.* **2014**, *10* (4), e1004038.

(56) Ayoglu, B.; et al. Autoantibody profiling in multiple sclerosis using arrays of human protein fragments. *Mol. Cell. Proteomics* **2013**, *12* (9), 2657–2672.

(57) Fagerberg, L.; et al. Analysis of the human tissue-specific expression by genome-wide integration of transcriptomics and antibody-based proteomics. *Mol. Cell. Proteomics* **2014**, *13* (2), 397–406.

(58) Tamura, T.; et al. The IRF family transcription factors in immunity and oncogenesis. *Annu. Rev. Immunol.* **2008**, *26*, 535–584.

(59) Wang, H.; Morse, H. C., 3rd. IRF8 regulates myeloid and B lymphoid lineage diversification. *Immunol. Res.* **2009**, *43* (1–3), 109–117.

(60) International Multiple Sclerosis Genetics Consortium.. The genetic association of variants in CD6, TNFRSF1A and IRF8 to multiple sclerosis: a multicenter case-control study. *PLoS One* **2011**, *6* (4), e18813.

(61) De Jager, P. L.; et al. Meta-analysis of genome scans and replication identify CD6, IRF8 and TNFRSF1A as new multiple sclerosis susceptibility loci. *Nat. Genet.* **2009**, *41* (7), 776–782.

(62) Yoshida, Y.; et al. The transcription factor IRF8 activates integrin-mediated TGF-beta signaling and promotes neuroinflammation. *Immunity* **2014**, *40* (2), 187–198.

(63) Romme Christensen, J.; et al. Cellular sources of dysregulated cytokines in relapsing-remitting multiple sclerosis. *J. Neuroinflammation* **2012**, *9*, 215.

(64) Liu, J.; et al. A METTL3-METTL14 complex mediates mammalian nuclear RNA N6-adenosine methylation. *Nat. Chem. Biol.* **2014**, *10* (2), 93–95.